Guest-Host Interactions in Sodium Zeolite Y: Structural and Dynamical ^{23}Na Double-Rotation NMR Study of H_2O, PMe_3, $Mo(CO)_6$, and $Mo(CO)_4(PMe_3)_2$ Adsorption in $Na_{56}Y$

Raz Jelinek,[†] Saim Özkar,[‡,§] Heloise O. Pastore,[§,∥] Andrej Malek,[§] and Geoffrey A. Ozin*[,§]

Contribution from the Materials Sciences Division, Lawrence Berkeley Laboratory and Department of Chemistry, University of California, Berkeley, California 94720, and Advanced Zeolite Materials Group, Lash Miller Chemical Laboratories, University of Toronto, 80 Saint George Street, Toronto, Ontario, Canada M5S 1A1. *Received May 13, 1992*

Abstract: ^{23}Na double-rotation NMR (DOR) provides site-specific structural and dynamical information on guest-host interactions within sodium zeolite Y pores. Quantitative adsorption of H_2O, PMe_3, and $Mo(CO)_6$ guests affects both the positions and line shapes of the ^{23}Na resonances from specific extraframework Na^+ sites. The evolution of the ^{23}Na DOR spectra with the progressive introduction of guest molecules allows one to probe direct "solvation" effects involving the Na^+ cations in the larger supercages, as well as indirect effects on the Na^+ cations in adjacent smaller sodalite cavities. ^{23}Na DOR experiments conducted at two magnetic field strengths confirm that PMe_3 coadsorption in $8\{Mo(CO)_6\},16\{PMe_3\}$-$Na_{56}Y$, and PMe_3 ligand-substitution in $8\{cis\text{-}Mo(CO)_4(PMe_3)_2\}$-$Na_{56}Y$ give rise to progressive deshielding and enhanced quadrupolar interactions of the anchoring Na^+ cations in the α-cages, relative to those of the starting material, $8\{Mo(CO)_6\}$-$Na_{56}Y$. Spin-lattice relaxation measurements indicate that adsorption of PMe_3 facilitates an increased motion of the Na^+ cations and/or guest species inside the α-cages.

Introduction

The most common extraframework charge-balancing cation found in as-synthesized zeolites is sodium.[1] Na^+ cations, located at specific sites within the zeolite lattice, play an important role in determining adsorption, chemical, and catalytic properties of zeolite Y. Understanding the interactions of the Na^+ cations with the zeolite framework and the guest species, their coordination, and their chemical characteristics is thus of great interest. However, direct methods for elucidating details concerning the individual extraframework sodium cations are usually neither straightforward nor unequivocal. In particular, conventional solid-state NMR studies of ^{23}Na nuclei in zeolites have had limited applications because of the large quadrupolar broadening present in the NMR spectra. The recent development of the double-rotation NMR (DOR) technique,[2] however, dramatically changes the situation for quadrupolar nuclei like ^{23}Na ($I = {}^3/_2$). By removing anisotropic line broadening contributions, DOR becomes a high-resolution spectral probe of structures, bonding, and dynamical effects involving ^{23}Na cation sites in zeolites. Recently, we have used ^{23}Na DOR to investigate cation-exchange processes in sodium zeolite Y,[3] and anchoring and oxidation reactions of molybdenum and tungsten hexacarbonyls within the supercages of the zeolite.[4]

In this work, ^{23}Na DOR is used for the first time to study the loading-dependent structural and dynamical consequences of adsorbing H_2O, $P(CH_3)_3$ (denoted PMe_3), and $Mo(CO)_6$ into dehydrated $Na_{56}Y$, as well as the coadsorption and substitution of CO ligands, by PMe_3 in $8\{Mo(CO)_6\}$-$Na_{56}Y$. Site-selective chemical shifts and quadrupolar parameters are obtained from ^{23}Na DOR measurements at two magnetic field strengths. Room temperature inversion-recovery experiments provide an estimate for the ^{23}Na longitudinal relaxation times, which yield additional information on motional effects of individual sodium cations and adsorbed guests.

Experimental Section

High-purity, crystalline zeolite Y, with $Na_{56}(AlO_2)_{56}(SiO_2)_{136}\cdot xH_2O$ unit-cell composition, was obtained from Dr. Edith Flanigen at UOP Corp. In order to remove cation defect sites, thermally dehydrated/calcined $Na_{56}Y$ was slurried with 0.01 M NaCl, 0.01 M NaOH solution and washed until free of Cl^-. All zeolite samples were stored over saturated NH_4Cl solution to ensure constant humidity until use. The thermal dehydration of $Na_{56}Y$, under dynamic vacuum ($\sim 10^{-5}$ Torr) using an Omega Series Model No. CN-2010 programmable temperature controller, follows a preset temperature schedule: 25-100 °C over 1 h, 1 h at 100 °C, 100-450 °C over 3 h, and 5 h at 450 °C. This was followed by calcination in a static atmosphere of 300 Torr of O_2 at 450 °C for 1 h and pumping at this temperature. The degree of dehydration was judged by the flatness of the baseline in the mid-IR ν-OH and δ-OH deformation regions, 3400-3700 and 1600-1650 cm^{-1}, respectively. Quantitative adsorption of H_2O and PMe_3 was achieved by exposing $Na_{56}Y$ to the gaseous materials, respectively. Preparation of the encapsulated $8\{Mo(CO)_6\}$-$Na_{56}Y$ and its PMe_3-substituted derivatives was achieved using techniques described previously.[5,6]

^{23}Na DOR experiments were carried out at 9.6- and 11.7-T magnetic fields on a Chemagnetics CMX-500 spectrometer using a home built probe whose features are described elsewhere.[7] The spinning speed was 5 kHz for the inner rotor and 600-800 Hz for the outer one. All samples were loaded into the air-tight sample spinners in a dry-argon glovebox. In each experiment, 1000-3000 acquisitions were accumulated. The one-pulse NMR experiments with 500-ms recycle delays used 4-μs (25°) pulses, while the inversion-recovery using the "soft" excitation pulses "sequence"[8] was used for measuring spin-lattice relaxation times. All spectra were zero-filled to 2K data points, with application of 200-Hz Lorentzian broadening. The external reference was 0.1 M NaCl solution.

Results and Discussion

H_2O and PMe_3 Adsorption. The framework of $Na_{56}Y$ consists of AlO_4^- and SiO_4 tetrahedra which form a face-centered cubic array of 6.6 Å diameter sodalite cavities. This arrangement creates a diamond network of larger 13 Å diameter supercages, of which there are eight in the cubic unit cell. A portion of this structure is shown in Figure 1. Extraframework, charge-balancing Na^+ cations are distributed among four different sites within the zeolite

* To whom correspondence should be addressed.
† University of California, Berkeley.
‡ On leave from the Chemistry Department, Middle East Technical University, Ankara, Turkey, 06531.
§ University of Toronto.
∥ Instituto de Quimica, Universidade Estadual de Campinas, Campinas, S.P., Brazil.

(1) Breck, D. W. *Zeolite Molecular Sieves*; R. E. Kieger Publishing Company: Malabar, FL, 1984.
(2) Wu, Y.; Chmelka, B. F.; Pines, A.; Davis, M. E.; Grobet, P. J.; Jacobs, P. A. *Nature* **1990**, *346*, 550.
(3) Jelinek, R.; Özkar, S.; Ozin, G. A. *J. Am. Chem. Soc.* **1992**, *114*, 4907.
(4) Jelinek, R.; Özkar, S.; Ozin, G. A. *J. Phys. Chem.* **1992**, *96*, 5949.
(5) Özkar, S.; Ozin, G. A.; Moller, K.; Bein, T. *J. Am. Chem. Soc.* **1990**, *112*, 9575.
(6) Ozin, G. A.; Özkar, S.; Pastore, H. O.; Poë, A. J.; Vichi, E. J. S. *J. Chem. Soc., Chem. Commun.* **1991**, 141. *Supramolecular Architecture*; ACS Symposium Series; American Chemical Society: Washington, DC, 1992; Vol. 499, p 314. Ozin, G. A.; Poë, A. J.; Pastore, H. O. *J. Am. Chem. Soc.*, in press.
(7) Wu, Y.; Sun, B. Q.; Pines, A.; Samoson, A.; Lippmaa, E. *J. Magn. Reson.* **1990**, *89*, 297.
(8) Vold, R. L.; Waugh, J. S.; Klein, M. P.; Phelps, D. E. *J. Chem. Phys.* **1968**, *48*, 3831.

0002-7863/93/1515-563$04.00/0

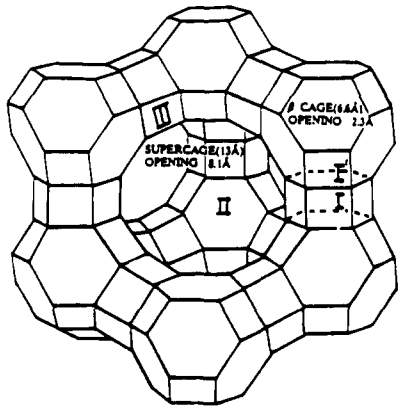

Figure 1. Illustration of part of the unit cell of sodium zeolite Y ($Na_{56}Y$). Extraframework cation sites I, I', II, and III are indicated.

lattice, as indicated in Figure 1. ^{23}Na DOR signals from specific sites within the zeolite framework were recently identified in our laboratories.[3]

^{23}Na DOR spectra of sodium zeolite Y loaded with known quantities of H_2O molecules are shown in Figure 2. The DOR spectrum of the dehydrated material (Figure 2a) features three distinct resonances at −4 ppm, −30 ppm, and −42 ppm which have been assigned to Na^+ cations at sites I, II, and I', respectively.[3] XRD and ND measurements have established that about 7–8% of the Na^+ cations in dehydrated $Na_{56}Y$ occupies the hexagonal prism site I, 24–33% is located inside the sodalite cage at site I', 53–57% is inside the supercage at site II, the remainder being either in the α-cage at site III or in an unknown position.[9] The DOR spectral intensities of the ^{23}Na peaks are evidently different from the population ratios determined by the XRD and ND experiments. The relatively small peaks assigned to Na^+ cations at site I', and in particular at site II, are partly due to a distribution of chemical environments which cause substantial broadening of the signals. Very broad spectral features might be lost in the baseline fluctuations as well as in spectrometer "dead-time", prior to the data acquisition.

Other factors determine the relative intensities observed in the DOR experiments and might account for the population ratio observed in the NMR spectra. It should be emphasized that in the NMR experiments which are carried out in this study, as well as in other systems which involve quadrupolar nuclei, what is observed, and mostly excited, is the "central transition" ($-^1/_2 \rightarrow {}^1/_2$). However, a certain amount of the excitation and resonance energies might account for "satellite transitions" of the quadrupolar nuclei ($-^3/_2 \rightarrow -^1/_2$ and $^1/_2 \rightarrow {}^3/_2$ for ^{23}Na nuclei), a situation which is denoted a "non-selective" excitation.[10] In some multisite materials, where some environments experience small quadrupolar interactions (such as the Na^+ cation at site I), while others exhibit greater quadrupolar effect (Na^+ cations at sites I' and II), the radio-frequency (rf) pulses might act differently on the nuclei. Specifically, nuclei that experience smaller quadrupolar interaction would exhibit greater spectral intensities than sites with high quadrupolar interaction, due to the effects of nonselective excitation of the spins.[10] This would produce spectra where the relative intensities will not correspond to an accurate population ratio of the sites.[11]

Another important issue which should be considered is the relative distribution of the NMR signal between the observed centerband and the spinning sidebands. The intensity incorporated in spinning sidebands in motional averaging experiments like MAS and DOR is determined by the spinning speed and also substantially by the anisotropic interactions present at the nuclei, such as the quadrupolar and anisotropic chemical shift.[12] In general,

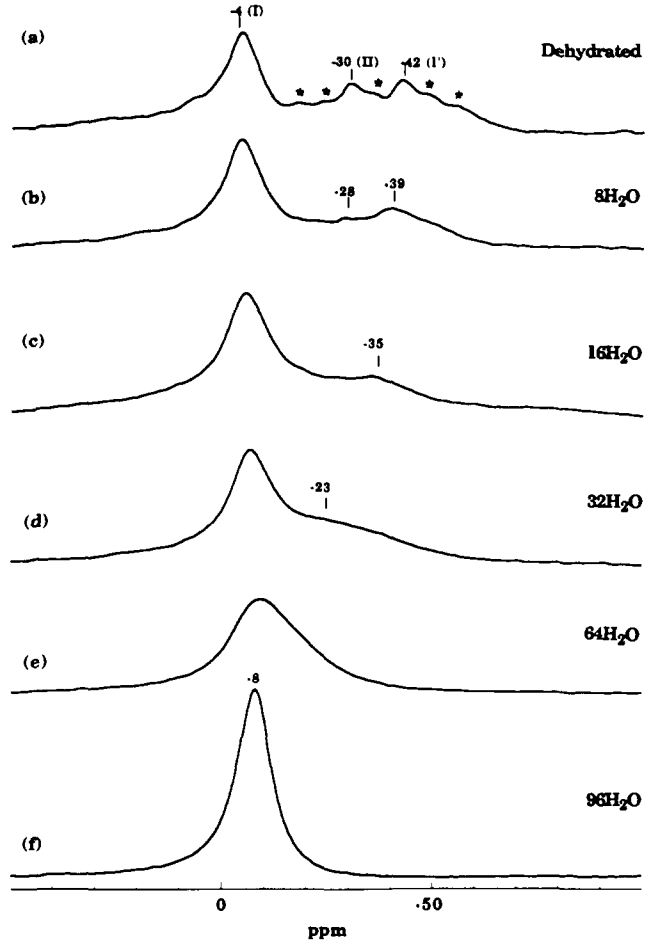

Figure 2. ^{23}Na DOR spectra at 11.7 T of (a) dehydrated $Na_{56}Y$ and of $Na_{56}Y$ progressively loaded with the following amounts of H_2O guest molecules: (b) 8 H_2O per unit cell; (c) 16 H_2O per unit cell; (d) 32 H_2O per unit cell; (e) 64 H_2O per unit cell; and (f) 96 H_2O per unit cell. * denote spinning sidebands.

more intensity will be transferred to spinning sidebands for nuclei which exhibit greater quadrupolar interactions. This is indeed demonstrated in Figure 2a. The peaks ascribed to Na^+ cations at sites I' and II are located within a broad sideband manifold. This stands in contrast to the ^{23}Na nuclei in the hexagonal prism at site I, which give rise to the sharp peak at around −4 ppm, with almost no associated spinning sidebands. The above effects contribute to the broad background signal and sideband manifold around −30 ppm in the ^{23}Na DOR spectrum of dehydrated $Na_{56}Y$ (Figure 2a) and limit the available information on population ratios that can be extracted from the intensities of the observed ^{23}Na DOR signals. Further discussion on intensity aspects in ^{23}Na DOR spectra of $Na_{56}Y$ is provided elsewhere.[3,4]

^{23}Na DOR spectra of partially hydrated $Na_{56}Y$ are shown in Figure 2b–e. As water molecules are progressively loaded into the cavities, a clear effect is detected on Na^+ cations at sites II and I'. The signals at −30 ppm and −42 ppm, ascribed to Na^+ cations at sites II and I', respectively, shift downfield, as more H_2O molecules are loaded, while the position of the peak at around −4 ppm, which is ascribed to Na^+ cations at site I, does not change upon water adsorption. Sites I' and II are located in the sodalite cage and the supercage, respectively (Figure 1), which are more spacious than the hexagonal prism, where site I is located. Thus, water molecules might penetrate the larger cages within the zeolite Y framework, causing the observed shifts in the resonance positions of Na^+ cations at sites I' and II (Figure 2b–e).

Previous studies have indicated that extraframework cations exhibit increased mobility in fully hydrated zeolite systems.[13,14]

(9) Fitch, A. M.; Jobic, H.; Renouprez, A. *J. Phys. Chem.* **1986**, *90*, 1311.
(10) Fenzke, D.; Freude, D.; Fröhlich, T.; Haase, J. *Chem. Phys. Lett.* **1984**, *111*, 171.
(11) Jelinek, R.; Chmelka, B. F.; Wu, Y.; Grandinetti, P. J.; Pines, A.; Barrie, P. J.; Klinowski, J. *J. Am. Chem. Soc.* **1991**, *113*, 4097.
(12) Maricq, M. M.; Waugh, J. S. *J. Chem. Phys.* **1979**, *70*, 3300.

The NMR results shown in Figure 2 are consistent with, and expand upon, this description. The quantitative adsorption of H_2O molecules in dehydrated $Na_{56}Y$ causes a progressive deshielding of the ^{23}Na nuclei at sites II and I′ (Figure 2) which likely arises from the combined effect of diminishing interactions with the framework oxygens and faster motion of the Na^+ cations. An interesting result is obtained for $Na_{56}Y$ zeolite which contains 32 H_2O molecules in the unit cell (Figure 2d). The profound downfield shift of the ^{23}Na peak ascribed to site I′, from −42 ppm to approximately −23 ppm, probably indicates a change of the interaction of site-I′ Na^+ cations with the zeolite framework. Migration of Na^+ cations from the sodalite cages to adjacent supercage sites might also contribute to the resonance shift; the migration is rendered feasible as the ionic diameter of Na^+ (2.3 Å[15]) is smaller than the six-ring opening between the sodalite cage and the supercage (2.7 Å[1]).

The sample that contains 96 H_2O molecules per unit cell features a narrower Gaussian signal at around −8 ppm (Figure 2f). This spectrum is essentially identical to the ^{23}Na DOR spectrum of the fully hydrated material $\{240H_2O\}$-$Na_{56}Y$ and indicates a single average environment for the Na^+ cations within the zeolite Y framework. The Na^+ cations are probably "solvated" by the water molecules at this stage and exhibit a very fast motion within the zeolite pores, on the time scale of the NMR experiments. The position of the ^{23}Na signal in Figure 2f, at around −8 ppm, is close to that of the observed resonance ascribed to site-I Na^+ cations inside the hexagonal prism, at around −4 ppm (Figure 2a). This indicates a highly symmetrical electronic environment for the hydrated Na^+ cations, due to the fast motion of the water molecules as well as the Na^+ cations.[13,16]

The observed mobilization of the extraframework Na^+ cations with progressive additions of H_2O molecules to $Na_{56}Y$ likely originates from coordination-number-dependent Lewis acid–Lewis base $\{H_2O\}\cdots Na^+OZ$ interactions. To check this proposal, we examined the adsorption effects of trimethylphosphine, a sterically large, soft (class B) Lewis base, compared to H_2O, a small, hard (class A) Lewis base. Binding of PMe_3 to Brønsted and Lewis acid sites in zeolite Y has been probed previously using ^{31}P MAS.[17,18] Figure 3 features the ^{23}Na DOR spectra of $Na_{56}Y$ zeolite quantitatively and progressively loaded with known amounts of PMe_3 guest molecules. The adsorbed PMe_3 guests clearly affect the environments of the ^{23}Na nuclei, causing profound changes in the positions and shapes of the sodium signals as shown in Figure 3.

Previous ^{31}P results indicate the occurrence of electronic interaction between the phosphorus atom of PMe_3 and Na^+ cations in the supercage of $Na_{56}Y$.[18] Indeed, the ^{23}Na DOR signal ascribed to site-II Na^+ cations is shifted downfield, from −30 ppm in dehydrated $Na_{56}Y$ (Figure 3a) to around −15 ppm upon loading 16 PMe_3 guest molecules (Figure 3c). A very interesting observation is the apparent effect of the adsorbed PMe_3 molecules on Na^+ cations at site I′, located inside the smaller sodalite cage (Figure 1). The ^{23}Na DOR peak at −42 ppm (Figure 3a), ascribed to Na^+ cations at site I′, shifts downfield to around −30 ppm upon PMe_3 loading. The kinetic diameter of PMe_3 is 5.5 Å,[19] significantly larger than the 2.7-Å-wide six-ring window of the sodalite cage. This does not permit incorporation of PMe_3 at room temperature into the sodalite cavities, unlike the H_2O guest molecules, as discussed above. The NMR results, shown in Figure 3b–e, show clearly that PMe_3 molecules, encapsulated within the α-cage, do

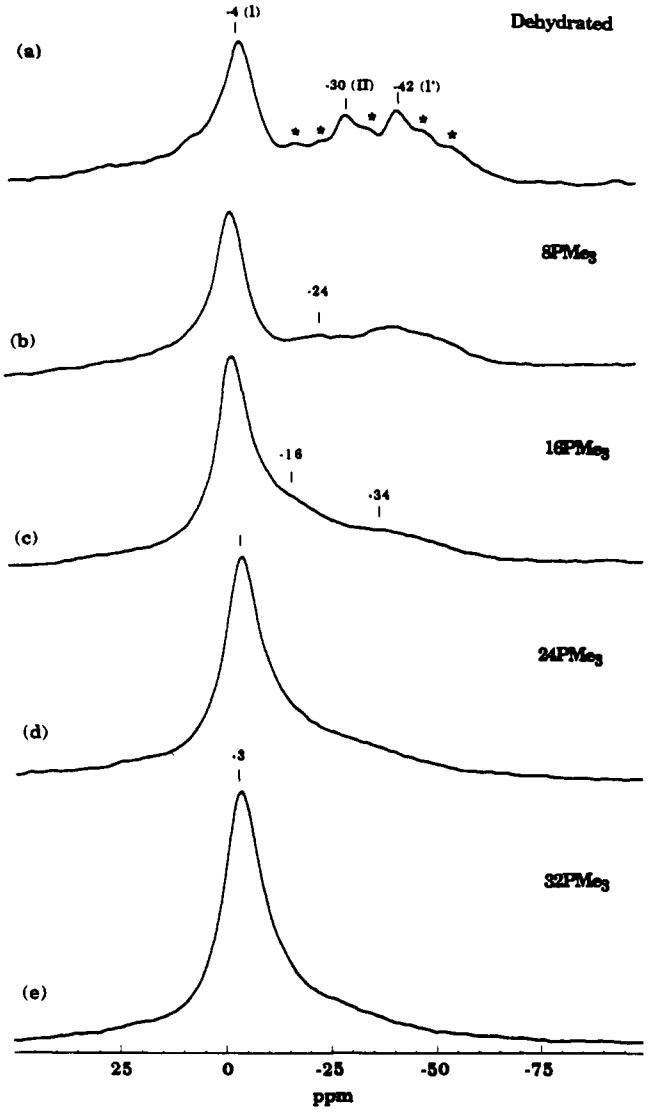

Figure 3. ^{23}Na DOR spectra at 11.7 T of (a) dehydrated $Na_{56}Y$ and of $Na_{56}Y$ progressively loaded with the following amounts of PMe_3 guest molecules: (b) 8 PMe_3 per unit cell; (c) 16 PMe_3 per unit cell; (d) 24 PMe_3 per unit cell; and (e) 32 PMe_3 per unit cell. ✱ denote spinning sidebands.

exhibit an indirect electronic (cooperative) effect on the smaller adjacent sodalite cavities. The downfield shift, as well as broadening of the ^{23}Na signal from site I′ in the sodalite cages, indicates a significant change of the environments of Na^+ cations at this site which might arise from an increased mobility of the Na^+ cations, as discussed above in the H_2O-loaded samples.

The highest-PMe_3-loaded $Na_{56}Y$ sample contains 4 PMe_3 guest molecules in a supercage. The ^{23}Na DOR spectrum of this material (Figure 3e) features a single Gaussian peak at around −3 ppm, which again indicates an average ^{23}Na environment. This observation favors a model of Na^+ cations coordinated by the mobile PMe_3, similar to the one proposed above for $Na_{56}Y$-containing adsorbed H_2O. The position of the ^{23}Na peak in the highest-loaded PMe_3 sample, at −3 ppm (Figure 3e), is detected further downfield from the analogous peak at −8 ppm (Figure 2f), ascribed to the Na^+ cations in the high-H_2O-loaded sample. This shift probably reflects differences in the nature of the interactions of the PMe_3 and H_2O guests, respectively, with the framework and Na^+ cations.

Note also the broad background signal observed at around −25 ppm for $\{32PMe_3\}$-$Na_{56}Y$ (Figure 3e). This feature is not detected in the ^{23}Na DOR spectrum of $\{96H_2O\}$-$Na_{56}Y$ (Figure 2f). This might indicate a more restricted motion of the Na^+ cations in the PMe_3-containing material, within and/or between the sodalites

(13) Tokuhiro, T.; Iton, L. E.; Peterson, E. M. *J. Chem. Phys.* **1983**, *78*, 7473. Lin, C. F.; Chao, K. J. *J. Phys. Chem.* **1991**, *95*, 9411.
(14) Jelinek, R.; Chmelka, B. F.; Stein, A.; Ozin, G. A. *J. Phys. Chem.* **1992**, *96*, 6744.
(15) Shannon, R. D. *Acta Crystallogr.* **1976**, *A32*, 751.
(16) Haase, J.; Park, K. D.; Guo, K.; Timken, H. K. C.; Oldfield, E. *J. Phys. Chem.* **1991**, *95*, 6996.
(17) Lunsford, J. H.; Rothwell, W. P.; Shen, W. *J. Am. Chem. Soc.* **1985**, *107*, 1540.
(18) Lunsford, J. H.; Tutunjian, P. N.; Chu, P.; Yeh, E. B.; Zalewski, D. J. *J. Phys. Chem.* **1989**, *93*, 2590.
(19) Zalewski, D. J.; Chu, P.; Tutunjian, P. N.; Lunsford, J. H. *Langmuir* **1989**, *5*, 1026.

and supercages, see above. Both effects might be related to steric limitations within the "crowded" supercages in {32PMe_3}-$Na_{56}Y$ and would cause broadening of the ^{23}Na signal.

Substitution of CO by PMe_3 in *n*{$Mo(CO)_6$}-$Na_{56}Y$. Recently, the first quantitative kinetic study for an archetypical substitution reaction of CO by PMe_3 in the well defined system *n*{$Mo(CO)_6$}-$Na_{56}Y$ has been reported.[6] Mixed first-order dissociative and second-order associative behavior of the encapsulated $Mo(CO)_6$ was observed. The results indicated a transition state which consists of an activated {$Mo(CO)_6$-$Na_{56}Y$}*, with PMe_3 anchored to Na^+ cations in the supercage of the $Na_{56}Y$ host lattice. Generally, an increase in PMe_3 loading produced a decrease in the activating ability of the host lattice and was attributed to deanchoring of the encapsulated complex, caused by $Me_3P\cdots Na^+OZ$, $Me_3P\cdots OZ$, and $Me_3P\cdots Me_3P$ interactions.

In order to achieve a more intimate understanding of the kinetics and mechanisms of these intrazeolitic ligand substitution reactions, we have employed ^{23}Na DOR to examine the reactant, *n*{$Mo(CO)_6$}-Na_{56}, the reactant-pair produced upon adsorption of PMe_3, *n*{$Mo(CO)_6$},*m*{PMe_3}-$Na_{56}Y$, and the kinetic product, *n*{*cis*-$Mo(CO)_4(PMe_3)_2$}-$Na_{56}Y$, all of which play key roles in the CO substitution of $Na_{56}Y$-encapsulated $Mo(CO)_6$ by PMe_3.[6]

The ^{23}Na DOR results, shown in Figure 4, yield additional insight into the loading-dependent anchoring interactions between the extraframework Na^+ cations and the adsorbed guest molecules. Introducing $Mo(CO)_6$ guests into $Na_{56}Y$ cavities causes a downfield shift of the ^{23}Na signal ascribed to site-II Na^+ cations, from −30 ppm in dehydrated $Na_{56}Y$ (Figure 4a) to around −24 ppm for 8{$Mo(CO)_6$}-$Na_{56}Y$ (Figure 4b). In addition, a significant increase in the intensity of the signal from Na^+ cations at site II is detected. These observations indicate a strong anchoring interaction between the $Mo(CO)_6$ guests and the site-II Na^+ cations in the supercage, through the oxygen-end of the carbonyl ligands. An extensive discussion concerning the intensity aspects in the ^{23}Na DOR spectra of $M(CO)_6$ species encapsulated in $Na_{56}Y$ is provided elsewhere.[3,4]

A further change in the environments of the extraframework Na^+ cations is detected in the ^{23}Na DOR spectrum of the intrazeolite reactant-pair, 8{$Mo(CO)_6$},16{PMe_3}-$Na_{56}Y$ (Figure 4c). Here, the addition of two PMe_3 guest molecules into a supercage containing one $Mo(CO)_6$ reactant molecule causes a downfield shift of the ^{23}Na signals associated with Na^+ at site II inside the supercage and site I′ located in the sodalite cavity. The positions of these two resonances in the spectrum of 8{$Mo(CO)_6$},16{PMe_3}-$Na_{56}Y$ are shifted downfield, to −20 ppm and −27 ppm, respectively, relative to those of the dehydrated $Na_{56}Y$ sample (Figure 4a) and the reactant 8{$Mo(CO)_6$}-$Na_{56}Y$ (Figure 4b). These results provide additional evidence for a direct electronic effect exerted by the PMe_3 guests on the site-II Na^+ cations anchored to the reactant $Mo(CO)_6$. The ^{23}Na DOR spectrum shown in Figure 4c also signals an indirect negative cooperative effect exerted by the PMe_3 guests on the Na^+ cations inside the adjacent sodalite cages. Recall that the smaller sodalite cavity is inaccessible to the PMe_3 molecules; however, a downfield shift is observed for the ^{23}Na DOR resonance associated with site-I′ Na^+ cations, inside the sodalite cage, from around −36 ppm for 8{$Mo(CO)_6$}-$Na_{56}Y$ (Figure 4b) to −27 ppm for 8{$Mo(CO)_6$},16{PMe_3}-$Na_{56}Y$ (Figure 4c).

The ^{23}Na DOR spectrum of the kinetic product, 8{*cis*-$Mo(CO)_4(PMe_3)_2$}-$Na_{56}Y$ (Figure 4d) features a noticeable difference from those of both the reactant (Figure 4b) and the reactant-pair (Figure 4c). The peak at −14 ppm in Figure 4d most likely corresponds to Na^+ cations at site II in the supercage. The site-II ^{23}Na resonance significantly shifts downfield, reflecting a different interaction between the encapsulated kinetic product *cis*-$Mo(CO)_4(PMe_3)_2$ and the extraframework Na^+ cations in the supercage, compared with the analogous interaction in the reactant $Mo(CO)_6$. This is consistent with the expectation that the oxygen-end of the anchoring *trans*-carbonyl ligands in 8{*cis*-$Mo(CO)_4(PMe_3)_2$}-$Na_{56}Y$ will exhibit a Lewis basicity higher than that in the reactant 8{$Mo(CO)_6$}-$Na_{56}Y$, due to the substitution of two CO ligands by PMe_3. The broad feature at around −35 ppm (Figure 4d) might arise from other ^{23}Na environments in the zeolite Y host, probably Na^+ cations within the sodalite cavities.

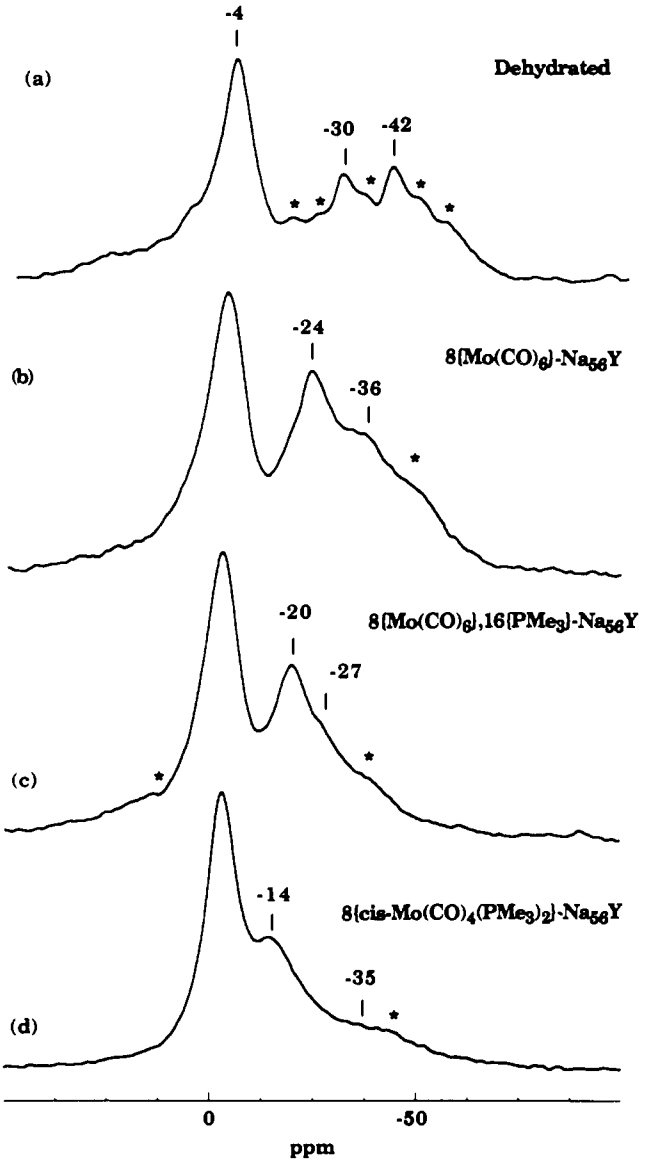

Figure 4. ^{23}Na DOR spectra at 11.7 T of (a) dehydrated $Na_{56}Y$ and of materials produced in the intrazeolite PMe_3 reactions of 8{$Mo(CO)_6$}-$Na_{56}Y$: (b) reactant material, 8{$Mo(CO)_6$}-$Na_{56}Y$; (c) reactant-pair, 8{$Mo(CO)_6$},16{PMe_3}-$Na_{56}Y$; (d) kinetic product, 8{*cis*-$Mo(CO)_4(PMe_3)_2$}-$Na_{56}Y$. * denote spinning sidebands.

Note that the ^{23}Na DOR resonance at around −4 ppm, ascribed to Na^+ cations at site I inside the hexagonal prism,[3] is not affected by the reactant, reactant-pair, or kinetic product contained in the supercages of $Na_{56}Y$ (Figure 4a–d). Na^+ cations at site I are spatially constrained between the two six-membered rings comprising the hexagonal prism (Figure 1), and therefore their interactions with the guest species inside the supercage are limited. Clearly, cooperative effects involving site-I Na^+ cations are negligible in these samples, as shown in Figure 4.

Further insight into the nature of the environments and interactions involving Na^+ cations in the supercages of $Na_{56}Y$ is provided by determining the chemical shift and quadrupolar contributions to the DOR lines. The centerband resonances that appear in DOR experiments, δ_{obs}, incorporate contributions from both the isotropic chemical shift, δ_{cs}, related to the charge density around the nuclei, and the isotropic second-order quadrupolar shift, $\delta_{Q,iso}$, as given by

$$\delta_{obs} = \delta_{cs} + \delta_{Q,iso} \quad (1)$$

Table I. Observed Positions of the ^{23}Na DOR Signal (δ_{obs}) Ascribed to Na^+ Cations at Site II in the Supercage of $Na_{56}Y$, at 11.7- and 9.6-T Magnetic Field Strengths, and Calculated Values for δ_{cs}, the Isotropic Chemical Shift, and $p_Q = (1 + (\eta^2/3))C_Q^2$, the Quadrupolar Product, Determined by Using Eqs 1 and 2[a]

	$8\{Mo(CO)_6\}$-$Na_{56}Y$	$8\{Mo(CO)_6\},16\{PMe_3\}$-$Na_{56}Y$	$8\{cis\text{-}Mo(CO_4)(PMe_3)_2\}$-$Na_{56}Y$
δ_{obs} (11.7 T), ppm	−24	−20	−14
δ_{obs} (9.6 T), ppm	−28	−24	−20
δ_{cs}, ppm	−16.9	−12.9	−3.3
p_Q, MHz	2.2	2.2	2.7

[a] The uncertainty in the peak positions was ±0.3 ppm.

$\delta_{Q,iso}$, the isotropic quadrupolar shift, is related to the magnetic field and the quadrupolar parameters by the equation

$$\delta_{Q,iso}\ (\text{ppm}) = -\frac{3[I(I+1) - 3/4]}{40I^2(2I-1)^2}\left(1 + \frac{\eta^2}{3}\right)\frac{C_Q^2}{\nu_0^2} \times 10^6 \quad (2)$$

where I is the nuclear spin, η is the asymmetry parameter, $C_Q \equiv e^2qQ/h$ is the quadrupolar coupling constant, and ν_0 is the resonance frequency. Thus, application of the DOR experiment in two magnetic field strengths enables one to determine independently the isotropic quadrupolar and chemical shift components of the observed resonances.[11]

Table I shows the positions of the ^{23}Na DOR signals ascribed to Na^+ cations at site II, at 11.7- and 9.6-T magnetic fields, and the calculated values of the isotropic chemical shift, δ_{cs}, and the quadrupolar product, $p_Q = (1 + (\eta^2/3))C_Q^2$, using eqs 1 and 2, respectively. The results reveal that, on passing from the reactant, $8\{Mo(CO)_6\}$-$Na_{56}Y$, to the reactant-pair, $8\{Mo(CO)_6\},16\{PMe_3\}$-$Na_{56}Y$, to the kinetic product, $8\{cis\text{-}Mo(CO)_4(PMe_3)_2\}$-$Na_{56}Y$, the primary effect is deshielding of the anchoring Na^+ cations at site II. This is entirely consistent with the notions of negative cooperative effects exerted by the PMe_3 guests in the reactant-pair, $8\{Mo(CO)_6\},16\{PMe_3\}$-$Na_{56}Y$, and the higher Lewis basicity of the oxygen-end of the carbonyl ligands in the kinetic product, $8\{cis\text{-}Mo(CO)_4(PMe_3)_2\}$-$Na_{56}Y$, both effects serving to modify the interaction and/or positioning of the Na^+ cations at their respective framework-oxygen six-membered-ring sites.

The calculations presented in Table I show that the quadrupolar product remains virtually unchanged, at 2.2 MHz, upon addition of PMe_3 to the reactant, $8\{Mo(CO)_6\}$-$Na_{56}Y$. This indicates a very small change in the electric field gradient around the ^{23}Na nuclei for the reactant pair. The quadrupolar product of the site-II ^{23}Na nuclei increases to 2.7 MHz on formation of the kinetic product, $8\{cis\text{-}Mo(CO)_4(PMe_3)_2\}$-$Na_{56}Y$, although this change might be statistically insignificant. This result, combined with the substantial deshielding of the ^{23}Na nuclei in the kinetic product (Table I), probably reflects a stronger anchoring of the *cis*-$Mo(CO)_4(PMe_3)_2$ molecules in the supercages of $Na_{56}Y$.

Spin–Lattice Relaxation Measurements. Valuable information on dynamical aspects concerning the motion of extraframework Na^+ cations, as well as the encapsulated guest species within the cavity spaces of sodium zeolite Y, can be obtained by estimating the spin–lattice relaxation times of the ^{23}Na nuclei. Relaxation of quadrupolar nuclei, such as ^{23}Na ($I = 3/2$), is dominated in diamagnetic systems by the interaction of the quadrupole moments with fluctuating electric field gradients.[20,21] The longitudinal relaxation of $I = 3/2$ nuclei due to the nuclear quadrupolar interactions should exhibit a nonexponential decay caused by a superposition of two exponentially decaying components.[20] In the extreme narrowing case, however, the quadrupolar spin–lattice relaxation time, $T_{1,Q}$, is given by[22]

$$(T_{1,Q})^{-1} = \frac{3\pi^2}{10}\left[\frac{2I+3}{I^2(2I-1)}\right]\left(\frac{e^2qQ}{h}\right)^2\left(1 + \frac{\eta^2}{3}\right)\tau_c \quad (3)$$

where τ_c is the correlation time characterizing the time dependence of the electric field gradient. Previous studies have related the time-dependent fluctuations of the electric field gradient around quadrupolar nuclei in fully hydrated zeolites to motion of water guest molecules and extraframework cations.[16,21]

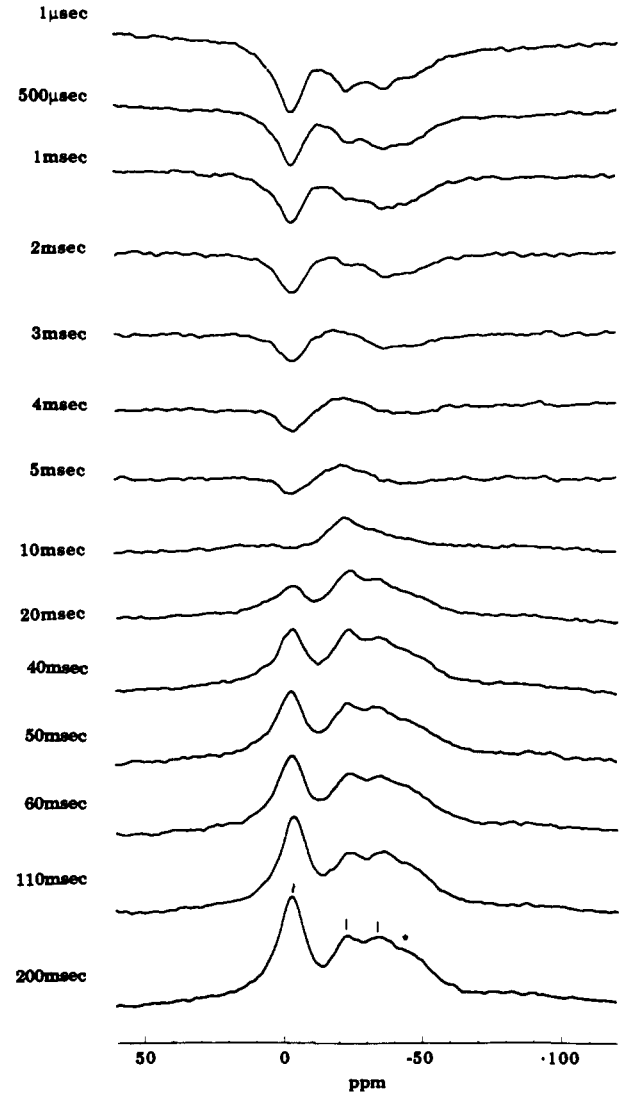

Figure 5. ^{23}Na DOR spectra of $8\{Mo(CO)_6\}$-$Na_{56}Y$ at 11.7 T, using the inversion–recovery pulse sequence, π–τ–$(\pi/2)$–detection. The delay time τ is indicated.

Figure 5 shows room temperature ^{23}Na DOR results of the reactant, $8\{Mo(CO)_6\}$-$Na_{56}Y$, for various values of delay time, τ, used in the inversion–recovery experiments [π–τ–$(\pi/2)$–detection]. Further spin–lattice relaxation experiments at variable temperatures are not yet feasible with our DOR apparatus. Inspection of the spectra shown in Figure 5 reveals that the ^{23}Na nuclei located at site I inside the hexagonal prism, which are associated with the ^{23}Na peak at around −3 ppm, exhibit longer spin–lattice relaxation than site-II Na^+ cations in the α-cage, which give rise to the upfield signal at around −24 ppm. The apparent slower spin–lattice relaxation of the site-I Na^+ cations might reflect the substantially smaller quadrupolar interaction experienced by the ^{23}Na nuclei at this site, which are located between two six-

(20) Hubbard, P. S. *J. Chem. Phys.* **1970**, *53*, 985.
(21) Haase, J.; Pfeifer, H.; Oehme, W.; Klinowski, J. *Chem. Phys. Lett.* **1988**, *150*, 189.
(22) Abragam, A. *Principles of Nuclear Magnetism*; Clarendon Press: Oxford, England, 1961.

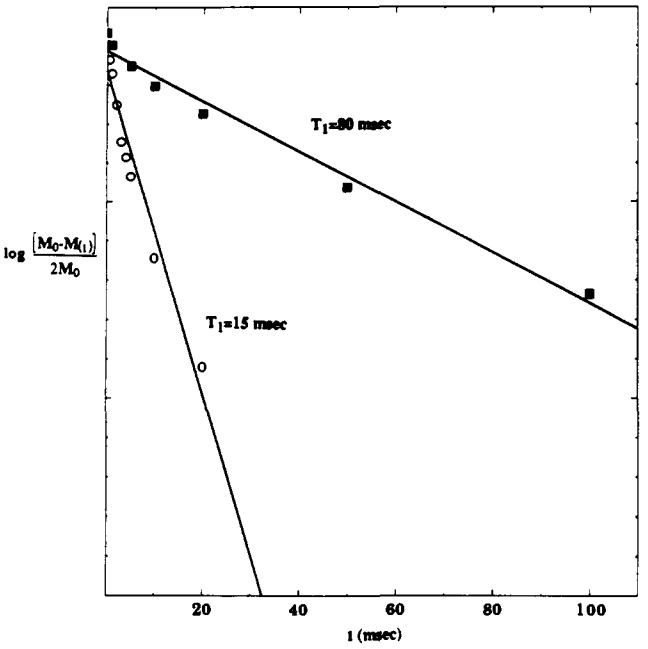

Figure 6. Semilogarithmic plot of the magnetization decay of the ^{23}Na nuclei at site II in the reactant, 8{$Mo(CO)_6$}-$Na_{56}Y$ (open circles), and the reactant-pair, 8{$Mo(CO)_6$},16{PMe_3}-$Na_{56}Y$ (shaded squares). M_0 is the peak intensity measured after more than $5T_1$ delay time, $M_{(t)}$ is the intensity measured in the inversion–recovery experiments at a particular delay time, t. The lines are the polynomial fittings of the experimental results. The T_1 values are the inverse of the respective slopes.

membered rings (Figure 1). Indeed, DOR experiments that were carried out at two magnetic field strengths yield a value of approximately p_Q = 0.4 MHz for the quadrupolar product of Na^+ cations at site I, compared to p_Q = 2.2 MHz for the ^{23}Na nuclei at site II (Table I).

Plots featuring the magnetization decays of the ^{23}Na nuclei at site II, in the reactant material, 8{$Mo(CO)_6$}-$Na_{56}Y$, and the reactant-pair sample, 8{$Mo(CO)_6$},16{PMe_3}-$Na_{56}Y$, are shown in Figure 6. The results indicate a significant increase in the longitudinal relaxation of the anchoring Na^+ cations at site II upon addition of PMe_3. The T_1 of the Na^+ cations at site II increases from around 15 msec, in the reactant, 8{$Mo(CO)_6$}-$Na_{56}Y$, to 80 msec, in the reactant-pair, 8{$Mo(CO)_6$},16{PMe_3}-$Na_{56}Y$ (Figure 6). The quadrupolar products p_Q of the ^{23}Na nuclei at site II are equal (Table I); therefore the increase of T_1 in the reactant-pair is most likely related to a *decrease* in the quadrupolar correlation time, τ_c (eq 3). This result is again consistent with the description of increased motion of the anchoring Na^+ cations, and/or the $Mo(CO)_6$ guest species, brought about by $Me_3P\cdots Na^+OZ$, $Me_3P\cdots OZ$, and $Me_3P\cdots Mo(CO)_6$ interactions in the supercage of $Na_{56}Y$. The increased mobility might produce faster fluctuations of the electric field gradients at the ^{23}Na nuclei, which will bring about the slower spin–lattice relaxation observed after the adsorption of the PMe_3 guest molecules.

Conclusions

This study provides a satisfying demonstration of the power of ^{23}Na DOR carried out at two magnetic field strengths, in combination with spin–lattice relaxation measurements, for elucidating site-specific structure, bonding, and dynamical details for extraframework Na^+ cations and a range of adsorbed guest molecules in sodium zeolite Y. Quantitative adsorption of H_2O and PMe_3 guests into $Na_{56}Y$ is found to affect Na^+ cations in both the spacious supercages and the smaller sodalite cages. PMe_3 molecules, which are only able to penetrate the supercages, exhibit a profound effect on Na^+ cations in adjacent sodalite cavities, either alone or coadsorbed with $Mo(CO)_6$ molecules.

By conducting the ^{23}Na DOR experiments at 11.7- and 9.6-T magnetic field strengths, one can determine the isotropic chemical shift and quadrupolar contributions to the DOR spectra. The results clearly indicate that coadsorbed PMe_3 guests in the reactant-pair, 8{$Mo(CO)_6$},16{PMe_3}-$Na_{56}Y$, and coordinated PMe_3 ligands in the product, 8{*cis*-$Mo(CO)_4(PMe_3)_2$}-$Na_{56}Y$, cause deshielding of the anchoring Na^+ cations inside the supercage. While the charge asymmetry around the ^{23}Na nuclei, which is reflected in the quadrupolar interactions, does not change on passing from the reactant to the reactant-pair, a small enhancement is observed in the more strongly anchored kinetic product.

Additional site-specific dynamical information is obtained by conducting ^{23}Na DOR spin–lattice relaxation experiments. The results indicate a slower longitudinal relaxation for ^{23}Na nuclei at site I, as compared to the site-II Na^+ cations, which might be related to the rather small quadrupolar interaction experienced by the Na^+ cations inside the hexagonal prism. A significant increase in T_1 of the Na^+ cations at site II in 8{$Mo(CO)_6$},16{PMe_3}-$Na_{56}Y$, compared to 8{$Mo(CO)_6$}-$Na_{56}Y$, probably reflects a faster motion of the guest molecules and/or extraframework Na^+ cations, caused by the coadsorption of PMe_3, which exhibits Lewis-base properties.

Acknowledgment. This work was supported by the Director, Office of Energy Research, Office of Basic Energy Sciences, Materials and Chemical Sciences Division, U.S. Department of Energy, under Contract No. DE-AC03-76SF00098. R.J. is grateful to Professor A. Pines for helpful discussions. G.A.O. wishes to acknowledge the Natural Science and Engineering Research Council (NSERC) of Canada's Operating and Strategic Grants Programmes.